J Mater Sci (2009) 44:4814–4826
DOI 10.1007/s10853-009-3734-y

Characterization of silicon phases in spray-formed and extruded hypereutectic Al–Si alloys by image analysis

Chengsong Cui · Alwin Schulz · Ellen Matthaei-Schulz · Hans-Werner Zoch

Received: 16 January 2009 / Accepted: 9 July 2009 / Published online: 22 July 2009

Abstract The silicon phases in the spray-formed and extruded hypereutectic Al–Si alloys (AlSi18, AlSi25 and AlSi35) have been quantitatively evaluated by means of image analysis technique. The influence of silicon content in the alloys, thermal conditions during spray forming of the alloys and hot extrusion of the spray-formed alloys on the size, shape, dispersion and orientation of the silicon phases have been studied and discussed. In general, the silicon phases are greatly refined and uniformly distributed in the spray-formed Al–Si alloys. This improvement in the silicon phases is further facilitated by low thermal input as well as fast cooling conditions during spray forming. The silicon particles in the as-extruded Al–Si alloys appear more homogeneous and regular than those in the as-deposited Al–Si alloys but exhibit a certain amount of anisotropy and a tendency to preferred orientation. The silicon particles, depending on the particle size and shape, may fracture or coarsen during extrusion.

Introduction

Hypereutectic aluminium–silicon alloys, with the features of low weight, high modulus, good wear resistance and low coefficient of thermal expansion, are attractive candidate materials for automotive, aerospace and electronics applications [1, 2]. Increasing silicon content in the alloys will further improve these properties. The hypereutectic Al–Si alloys have been produced by casting methods, but in practice they are not applied. The main reason is that they contain coarse primary silicon particles which give a product with poor machinability, hot workability and mechanical properties [3, 4]. Addition of a modifier containing phosphorus for refining the primary silicon particles is unsatisfactory, especially when the hypereutectic Al–Si casting alloy contains 25 wt% or more of silicon [5].

Spray forming, a relatively new metallurgical process with the characteristics of rapid solidification and near net shape production, has been considered to be suitable for the manufacture of such materials [6, 7]. According to this method, the hypereutectic Al–Si alloys with well-refined primary silicon particles can be obtained, even if they contain more than 25 wt% silicon [8–12]. Compared with other competitive methods, for example, powder metallurgy, the spray forming process is more promising because it has the advantages of single-step operation from molten alloy to a consolidated product and therefore lower oxygen content and lower production cost [7, 8].

Hypereutectic Al–Si alloys can be regarded as composite materials, in which silicon phases act as reinforcement in the α-aluminium matrix. Since the properties and performances of particulate-reinforced composites strongly depend on the size, shape, interparticle spacing and volume fraction of the particles [13], characterization and evaluation of the silicon phases in the spray-formed hypereutectic Al–Si alloys are of great interest and importance. In addition, the influence of thermal conditions during spray forming and subsequent hot working on the silicon phases also need to be investigated, because the microstructures of the spray-formed materials may differ considerably under different processing conditions. So far, a large number of studies on the spray forming of hypereutectic Al–Si alloys have been carried out, but quantitative evaluation of the silicon phases in the as-deposited and hot worked materials

C. Cui (✉) · A. Schulz · E. Matthaei-Schulz · H.-W. Zoch
Foundation Institute of Materials Science, Badgasteiner Str. 3, 28359 Bremen, Germany
e-mail: cscui@iwt.uni-bremen.de

is rarely reported. In this study, the silicon phases in a variety of spray-formed and extruded hypereutectic Al–Si alloys are quantitatively evaluated by means of image analysis technique. Since the commercial cast hypereutectic Al–Si alloys generally contain 18 wt% Si (e.g. 390 alloy) and the commercial spray-formed hypereutectic Al–Si alloys generally contain 25 wt% Si, these two Si levels have been selected for the Al–Si hypereutectic alloys in this study. In addition, hypereutectic Al–Si alloys containing higher silicon are of great interest, thus a Si level of 35 wt% has also been selected. The influence of silicon content in the alloys, thermal conditions during spray forming of the alloys and hot extrusion of the spray-formed alloys on the size, shape, dispersion and orientation of the silicon phases have been studied and discussed.

As the alloys studied are hypereutectic Al–Si alloys, one would assume that the primary silicon particles are the ones of interest in this article. However, as eutectic silicon phase particles are also present in the microstructures and they are generally modified into short and blunted particles or grow epitaxially on the primary silicon phase [14, 15], it is difficult to distinguish between the two types. Consequently, in this study, the two types of silicon phases are grouped together for characterization purposes.

Experimental

Material preparation

Three hypereutectic Al–Si alloys containing 18, 25 and 35 wt% silicon were selected as the experimental materials. The molten alloys with a superheat of 75 K were atomized by a scanning free-fall atomizer and spray deposited on a rotating substrate, resulting in cylindrical billets. The atomization gas pressure and the diameter of the pouring nozzle for the melts were adjusted to achieve different thermal conditions of the deposited materials during spray forming; accordingly different microstructures of the spray-formed alloys were obtained. The main process parameters for the representative spray-formed Al–Si alloys studied in this article are listed in Table 1. For each alloy, the billets spray formed under comparatively hot conditions and comparatively cold conditions were used for further investigation. More details of the spray forming procedures can be found in Refs. [17].

To eliminate the porosity in the deposits and prepare semi-finished materials for subsequent applications, the spray-formed billets usually need to be hot worked. In this study, the spray-formed Al–Si alloy billets (107 mm diameter and max. 345 mm length after machining) were heated in an induction furnace to a temperature of 460–470 °C and extruded by means of indirect extrusion to wires in an experimental 8 MN press at the Extrusion Research and Development Center of the Technical University of Berlin. The wires are supposed to be further cold drawn into thin wires ($\sim$1.2 mm diameter) as filler materials for laser beam welding of aircraft structures [17]. For the billet V334, five wires with a diameter of 6 mm were simultaneously extruded with an extrusion ratio of 67. For the other billets, only one wire with a diameter of 8 mm was extruded from each of the billets with an area reduction ratio about 189. The ram speed was in the range of 0.5–0.7 mm/s, and the extrusion force was in the range of 3.5–5.0 MN. More details of the extrusion procedures can be found in Refs. [17].

The samples metallographically prepared for image analysis were obtained from the spray-formed deposits and the extruded wires. The samples show typical microstructures of the materials. No etching is required, as silicon appears grey, while the alpha-Al phase appears white under the light microscope for image analysis.

Table 1 Main spray forming parameters for hypereutectic Al–Si alloys

Alloy	Exp. no.	Melting temperature (°C)	Atomization gas pressure (MPa)	Pouring nozzle diameter (mm)	Spray distance (mm)	GMR	Thermal condition[b]
AlSi18	V457	732	0.4	4.0	440	4.0	Hot
	V334[a]	732	0.4	4.0	500	>4.0	Cold
AlSi25	V458	823	0.4	4.0	440	4.0	Hot
	V488	823	0.5	4.0	440	7.4	Cold
AlSi35	V460	953	0.4	4.5	440	5.3	Hot
	V487	953	0.6	4.0	440	7.7	Cold

[a] Serious nozzle freezing happened in the spray forming process of V334, thus the melt flow rate was much lower than the desired value, resulting in high GMR and cold spray condition

[b] The "hot" or "cold" thermal condition is qualitative and relative definition, depending on the thermal input and cooling condition in spray forming. The thermal input is subject to the melting temperature and the enthalpy of the spray-formed alloys. The cooling condition is dominated by the important parameter GMR (the ratio between the gas mass flow rate and the melt mass flow rate)

Image analysis

The image analysis of the silicon phases were made with the program Leica QWin V3.2.1 [18] on a light microscope Leica DMRX with a Prior-scan table, a camera Sony DXP-950 with a resolution of 768 × 574 pixels. For AlSi18 and AlSi25, the measurements of the silicon particles were performed with a ×100 objective (calibration 0.081 μm/pixel). For AlSi35 with large silicon particles, the measurements were made with ×50 and ×20 lens (calibration 0.163 and 0.412 μm/pixel). For each sample, the measurements were made at four positions, each measuring 5 × 5 fields with a field size of 57 × 42 μm^2 for AlSi18 and AlSi25 (×100 objective), and 114 × 83 μm^2 (×50 objective) and 291 × 211 μm^2 (×20 objective) for AlSi35.

The digital image processing of the grey images was adapted as necessary to achieve good mappings of the objects (silicon phase, pores) of interest concerning area and shape. Pores and silicon particles can be distinguished by grey value. The particle edges' determination is enhanced using delineation procedures [18]. For determination of the total content of silicon phase, no limits for particle size were set. For the analysis of particle geometry, a minimum particle size of 8 pixels was applied. The shape of the silicon particles is not spherical, but appears more complex and irregular; therefore, the particles which may be agglomerated were not segmented because the boundaries where to separate the particles were not clearly defined.

Quantitative measures

Silicon content

According to stereological theory [19], the area fraction of a microstructure measured on a two-dimensional section is equal to the volume fraction if the microstructure is distributed homogeneously within the sample volume. Therefore, the area fraction of the silicon phase was determined over large sample areas by field measurements. This means no particles were cut by the image boundary and no limits of particle size were set. A mean value was calculated over the values obtained from all measured fields. From the area and volume fraction of the silicon phase, the silicon content in mass percentage was calculated with a density of 2.7 g/cm^3 for aluminium and 2.33 g/cm^3 for silicon.

Areal density of silicon particles

The silicon particles in the measured fields were counted by the use of the Leica Qwin program. From this particle counting the quantity of the silicon particles per square millimetre can be calculated.

Size factor

A particle size factor is a number referring to how big a particle is. For spherical particles, the size of which are adequately represented by their diameters. For nonspherical particles, there are a variety of ways to express their sizes, for example, Feret's diameter, Martin's diameter and so on [20]. Any of the parameters can only reflect part of the size of a particle in irregular shape.

In this study, the longest Feret diameter, hereby defined as the measured length L, is used to characterize the size of silicon particles (see Fig. 1). In addition, another term equivalent diameter d_{eq} is also used to evaluate the silicon particle size, as given by

$$d_{eq} = \sqrt{\frac{4A}{\pi}} \quad (1)$$

where A is the area of a silicon particle. This parameter gives the diameter of a circle with the same area of the particle.

Shape factor

A shape factor is a number characterizing the shape of a particle. One of the shape factors known as aspect ratio φ is defined as the ratio of the length L (the longest Feret) to the breadth W (the shortest Feret) of the particle and reflects its elongation [21, 22].

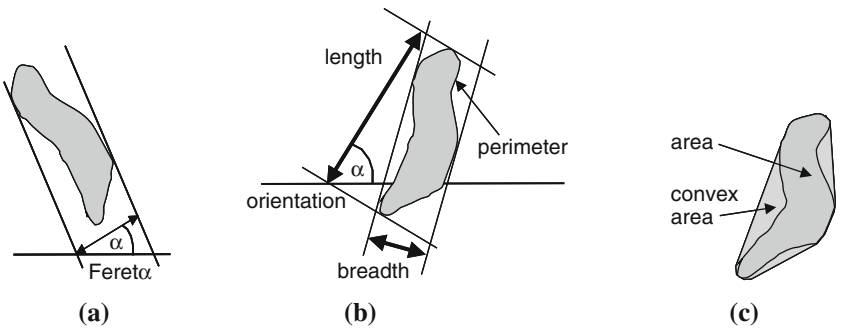

Fig. 1 Definition of parameters for characterization of silicon phases in an image

$$\phi = \frac{L}{W} \tag{2}$$

Another shape factor, here defined as roundness, is based on the cross-sectional area A and the perimeter P of the particle [21, 22]:

$$R = \frac{P^2}{4\pi A} \quad \in [1, \infty] \tag{3}$$

which describes the form of the particle and will be 1 for a circle and increases with more complex geometries.

A third shape factor used in the study is called bulging or fullness ratio, which reflects the part of coverage of the cross section of the particle with respect to the convex profile of its boundary and gives an estimate of the complexity of geometry (a measure of particle convexity and solidity) [21, 23]:

$$F = \sqrt{\frac{A}{A_c}} \tag{4}$$

where A_c is the area within the convex perimeter of the particle.

These shape factors are the most commonly used shape parameters which best describe granules [22]. These parameters all assume a value of 1 for a sphere. Fullness ratio is mainly related to surface regularity of the particle, aspect ratio to particle geometry and roundness to both of them [23].

Dispersion factor

Despite size and shape, the dispersion of the silicon particles is also considered in this study. The mean free path (MFP) d_{MFP} gives the average interface-to-interface distance between the silicon particles (including eutectic phase) and can be calculated according to [24]

$$d_{MFP} = \pi \cdot (1 - A_T) \cdot \frac{A_{field}}{P_T} \tag{5}$$

where A_T is the area fraction of all particles within one measured field, A_{field} is the area of the measured field and P_T is the sum of perimeters of all particles in the measured field.

Anisotropy factor and orientation

The anisotropy factor V/H is the ratio of the sum of all chord lengths in vertical (extrusion direction) and horizontal directions of the image over all particles on the whole in one measured field. It is determined as one mean value per image.

The orientation of each silicon particle is also determined. The angle α between the longest Feret diameter and the horizontal direction of the image gives the orientation of the particle (see Fig. 1b).

Definitions of the parameters for characterization of silicon phases in an image are illustrated in Fig. 1. More details of the characterization methods can be found in Ref. [16].

Results and discussion

Microscopic images

The microstructures of the as-deposited hypereutectic Al–Si alloys, which are spray formed under different thermal conditions, are shown in Fig. 2 (the upper half). The spray-formed hypereutectic Al–Si alloys are typically composed of refined primary silicon and modified eutectic. The silicon particles in the AlSi18 deposits and the AlSi25 deposits are very fine, like granule or particulate in shape. The silicon particles in the AlSi35 deposit prepared under the relatively cold spray conditions are also well refined. In contrast, large primary silicon particles, together with acicular eutectic phase, are still present in the AlSi35 deposit prepared under the comparatively hot spray conditions. In spite of this, the silicon particles in the as-deposited hypereutectic Al–Si alloys are much smaller than those in the corresponding cast alloys [25]. The distribution of the silicon particles in the spray-formed alloys is also much more homogeneous than that in the cast materials. These characteristics of the spray-formed Al–Si alloys can be attributed to copious nucleation in the melt during rapid cooling in flight and on deposition, the deformation and fragmentation experienced by the partially solidified droplets on impact, and remelting of the solid component in the top surface region of the deposit [11]. Epitaxial growth of eutectic silicon on the pre-existing primary silicon may also contribute to the modification of the eutectic phase [14].

Qualitatively speaking, the silicon particle size increases with increasing silicon content in the spray-formed Al–Si alloys under similar thermal conditions. The cooling rate of the deposited materials also greatly influences the size of the silicon particles. The faster the cooling rate is, the smaller the silicon particles are. Since the silicon particles are in irregular shape, without the use of image analysis, it is difficult to describe the differences in the morphology, dispersion and orientation of the silicon particles in the spray-formed Al–Si alloys.

Figure 2 (the lower half) also shows the microstructures of the extrusions from the spray-formed hypereutectic Al–Si alloys (longitudinal sections). The appearance of the silicon phases is similar to that of the as-deposited phases, but the acicular eutectic phase in the hot-sprayed AlSi35 deposit disappears in the extrusion. The extremely fine

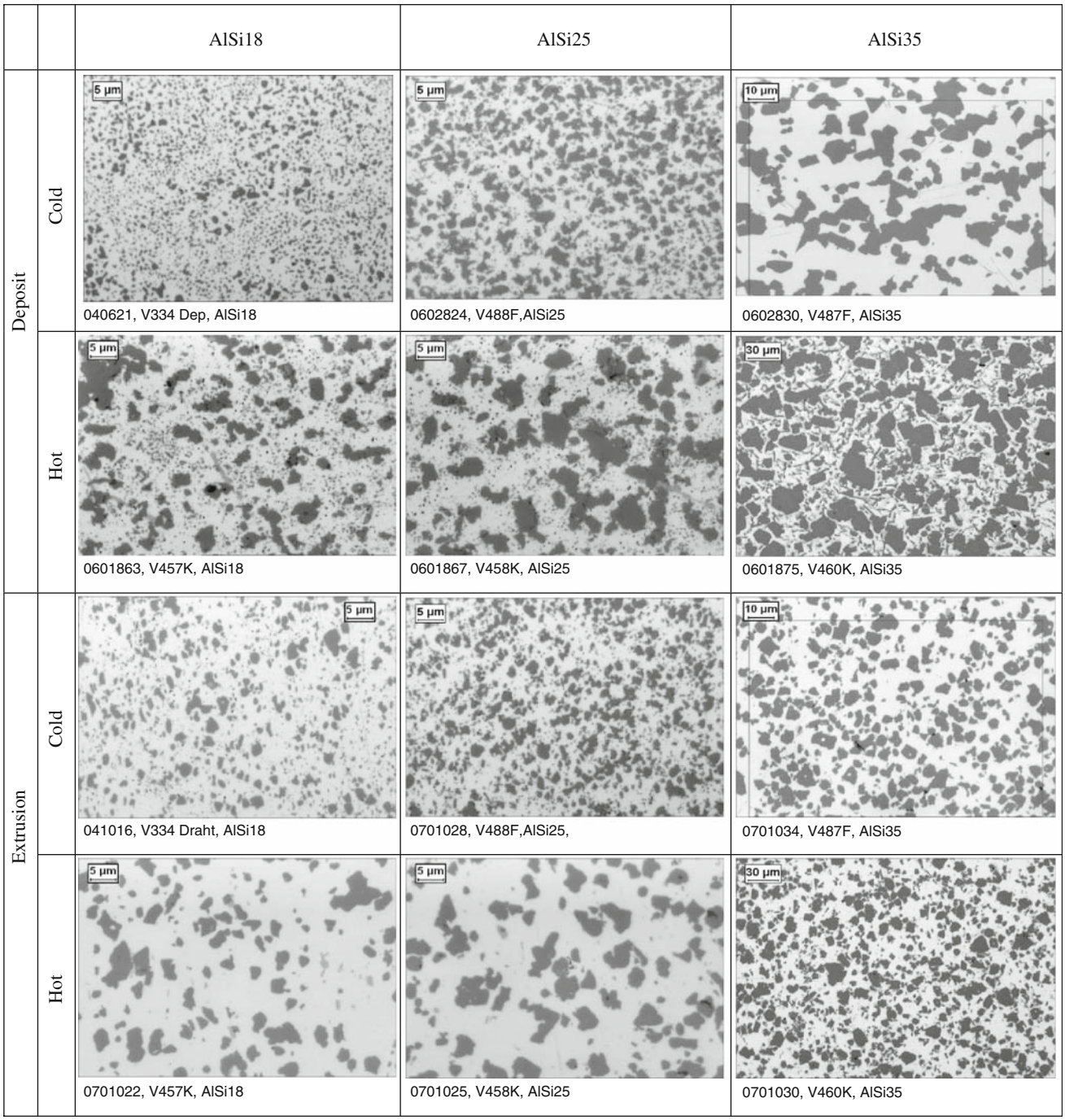

Fig. 2 Micrographs of silicon phases in the as-deposited and as-extruded hypereutectic Al–Si alloys spray formed under different thermal conditions

particles in the as-deposited AlSi18 and AlSi25 alloys seem to diffuse to the large particles during extrusion. The size of the primary silicon particles in the AlSi35 deposits decreases considerably after extrusion. The distribution of the silicon particles looks more homogeneous in the as-extruded alloys than in the as-deposited alloys.

Silicon content

Figure 3 presents the silicon contents, measured by means of image analysis, of the as-deposited Al–Si alloys prepared under different thermal conditions and the corresponding as-extruded Al–Si alloys. The measured results

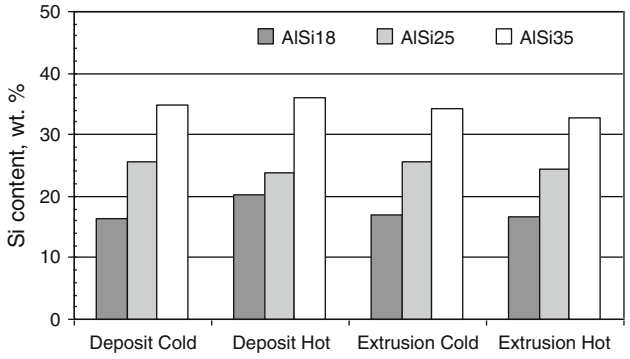

Fig. 3 Silicon contents in the as-deposited and as-extruded hypereutectic Al–Si alloys spray formed under different thermal conditions

are close to the nominal composition of the alloys. The measurement errors are probably caused by the resolution of the images for image processing.

Quantity of silicon particles

Figure 4 shows the quantity of the silicon precipitates in the as-deposited Al–Si alloys spray formed under different thermal conditions and the corresponding as-extruded alloys. Cold spray conditions (high cooling rates of the deposits) lead to high nucleation rates and therefore a large number of silicon precipitates. However, the number of the particles in the hot-sprayed AlSi35 deposit is slightly higher than that in the cold-sprayed AlSi35 deposit due to the counting of the eutectic phase. Fragmentation and remelting of the precipitates at the top surface of the cold-sprayed deposit further help to increase the quantity of silicon particles.

The quantity of the silicon particles in the deposits decreases with increasing silicon content. This can be explained by the high enthalpy input associated with the high silicon alloys. As the silicon content increases, the change of enthalpy from the preheating temperature to the

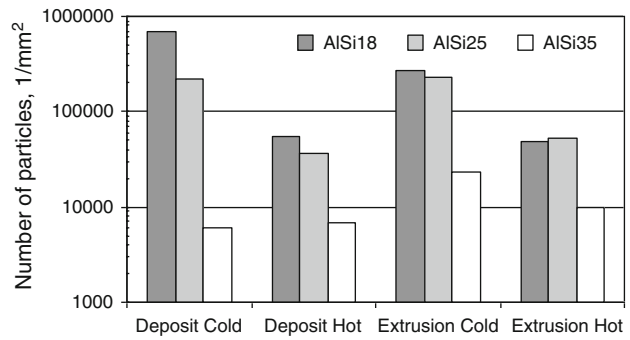

Fig. 4 Quantity of silicon precipitates in the as-deposited and as-extruded hypereutectic Al–Si alloys spray formed under different thermal conditions

end of solidification increases considerably. In comparison with the AlSi18 alloy, the corresponding enthalpy changes for the AlSi25 and AlSi35 alloys increase by 25 and 61%, respectively [16, 26]. This means during solidification much more heat needs to be released from the high silicon alloys in comparison with the low silicon alloys. Under similar cooling conditions during spray forming, high silicon alloys will undergo relatively slow cooling and solidification, resulting in relatively small quantity of nucleation centres and silicon precipitates. Besides, coarsening of silicon particles in the high silicon alloys is also facilitated by the slow solidification process. Since small particles may coarsen while large particles may fracture during hot extrusion, the quantity of the silicon particles decreases in the extruded AlSi18 alloy but increases in the extruded AlSi35 alloy.

Size and shape of silicon particles

The size and shape of the silicon particles in the as-deposited Al–Si alloys and the as-extruded alloys are shown in Fig. 5. The median values d50 of the particle size and the particle shape factors, as well as the d16 and d84 values of the measurements given by the scatter bars, are plotted in the diagrams. Due to the presence of a large amount of extremely fine particles, the median length (the longest Feret) and the median equivalent diameter of the silicon particles are very small (less than 2 μm for the AlSi18 and AlSi25 alloys, and less than 10 μm for the AlSi35 alloy). The difference in particle size between the AlSi18 and AlSi25 alloys is not obvious. The length and the equivalent diameter of the AlSi35 alloy are larger than those of the AlSi18 and AlSi25 alloys. The hot spray conditions lead to larger particle size, although the increase in value is very small. The influence of hot extrusion on the particle size is not clearly seen.

The aspect ratio of the silicon particles is around 1.6, with a large scatter of data. This means the silicon particles generally have an elongated shape. The influence of silicon content, thermal conditions and extrusion on this parameter is not clear. The roundness ratios of the particles in the Al–Si alloys prepared under different processing conditions lie in the same range, except that the hot-sprayed deposits show slightly high values. The bulging effect of the particles is in the same range, except the slightly low values of the hot-sprayed deposits. These results indicate that the silicon particles in the hot-sprayed deposits are more irregular than rounded.

Size and shape of primary silicon particles

It is seen in the above evaluation that the median particle size of the spray-formed Al–Si alloys is very small when the extremely fine particles are taken into account.

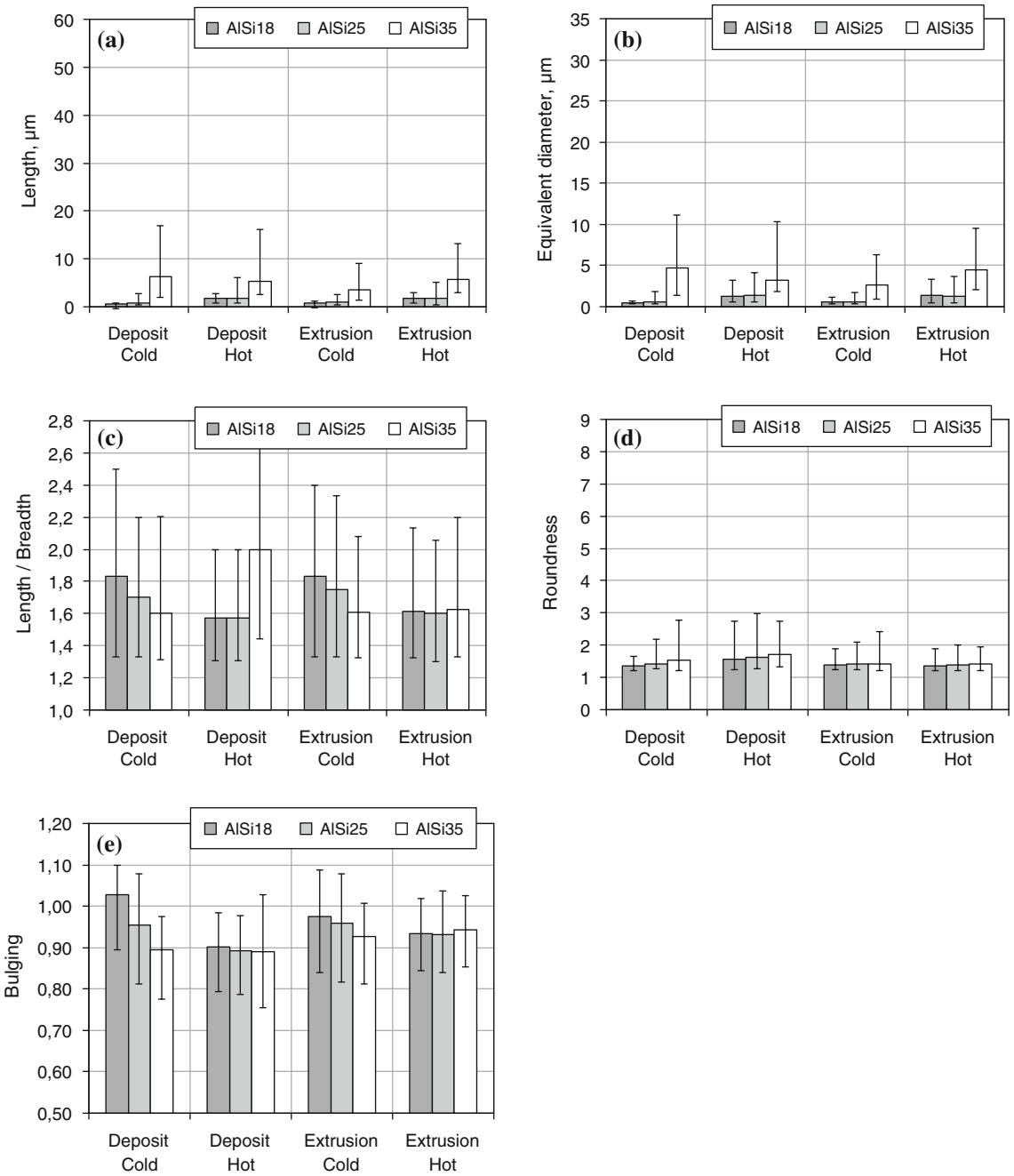

Fig. 5 Comparison of size and shape of all silicon particles in the as-deposited and as-extruded hypereutectic Al–Si alloys spray formed under different thermal conditions: **a** length, **b** equivalent diameter, **c** aspect ratio, **d** roundness, **e** bulging

Obviously, this evaluation cannot effectively reflect and compare the size of the silicon phases under different processing conditions because the difference in particle size is clearly seen in the microscopic images.

The typical microstructure of a cast hypereutectic Al–Si alloy consists of coarse primary silicon plates and α-Al/Si eutectic lamellar [27]. The amount of the two types of phases can be determined according to the phase diagram of binary Al–Si alloys. For the three alloys studied in this study, the contents of primary silicon and eutectic silicon are listed in Table 2. In microscopic images, different phases can be identified in terms of their shapes and colours. However, it is difficult to separate completely the eutectic silicon from the primary silicon in the spray-formed hypereutectic Al–Si alloys, because the eutectic phase is normally modified into short and blunted particles or grows epitaxially on the primary silicon phase. In this study, for simplification, a critical size is defined to classify

Table 2 Theoretical contents of primary silicon and eutectic silicon in hypereutectic binary Al–Si alloys

	Primary Si		Eutectic Si		Sum	
	wt%	vol.%	wt%	vol.%	wt%	vol.%
AlSi18	6.3	7.1	11.7	13.2	18	20.3
AlSi25	14.3	16.0	10.7	12.0	25	28.0
AlSi35	25.7	28.3	9.3	10.2	35	38.5

the two phases. For a hypereutectic Al–Si alloy, the total volume of the particles larger than this size is equal to the theoretical volume of primary silicon in the alloy. Accordingly, the particles larger than the critical size are classified as primary particles. Although this classification of the primary phase needs to be further discussed, this provides an approach to characterize the large particles, mostly the primary silicon phase.

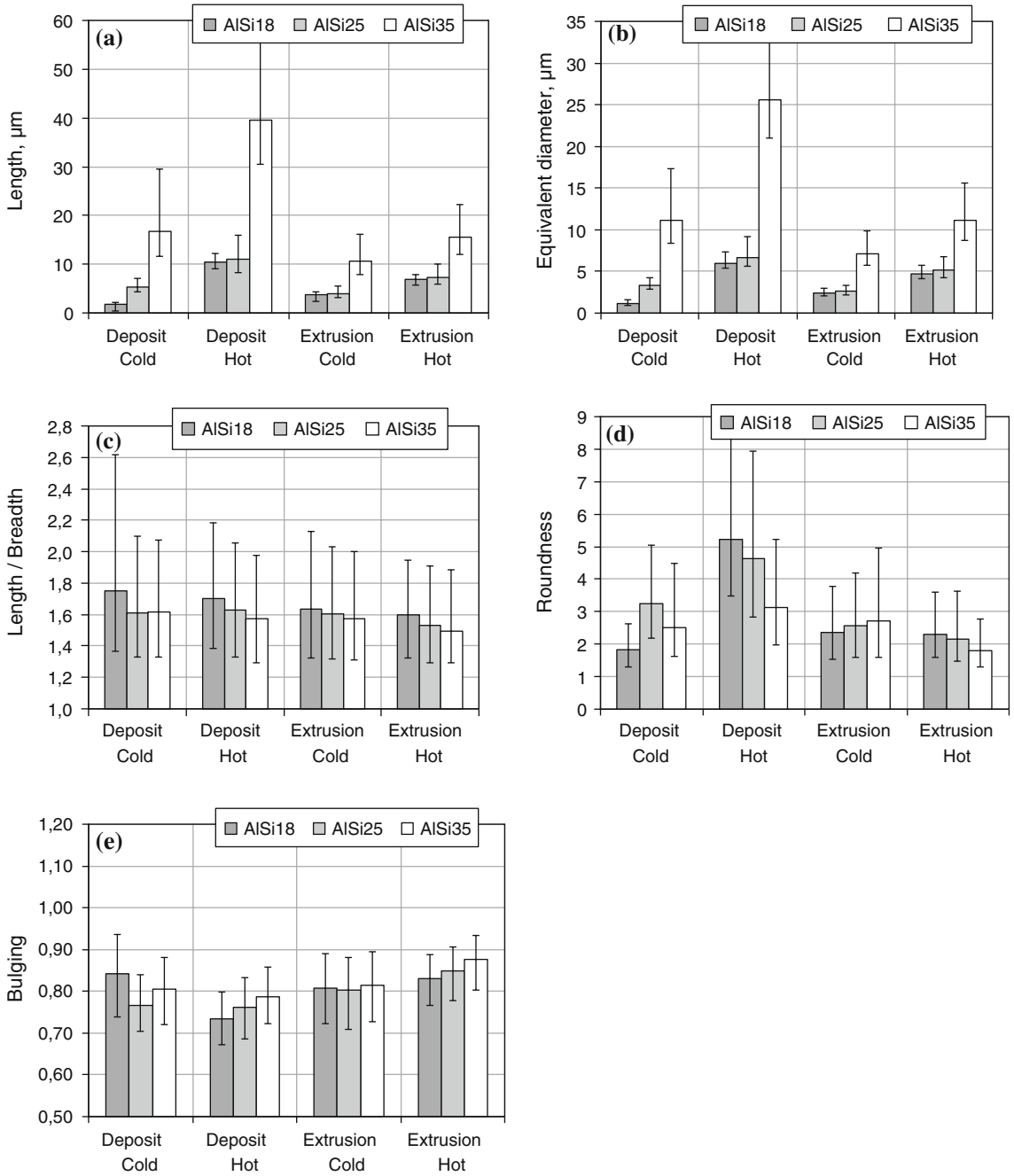

Fig. 6 Comparison of size and shape of primary silicon particles in the as-deposited and as-extruded hypereutectic Al–Si alloys spray formed under different thermal conditions: **a** length, **b** equivalent diameter, **c** aspect ratio, **d** roundness, **e** bulging

In this section, the evaluation of the size and shape of primary silicon particles is performed only with the silicon particles larger than the critical size. The size and shape factors of the primary silicon particles in the as-deposited hypereutectic Al–Si alloys and the corresponding as-extruded alloys are shown in Fig. 6.

The median length d50 of the primary particles in the cold-sprayed AlSi18, AlSi25 and AlSi35 deposits is approximately 2, 5 and 17 μm, respectively. Apparently, as the silicon content increases, the particle size as well as the data scatter also increases. In the hot-sprayed deposits, the median particle length of the AlSi18 deposit and the

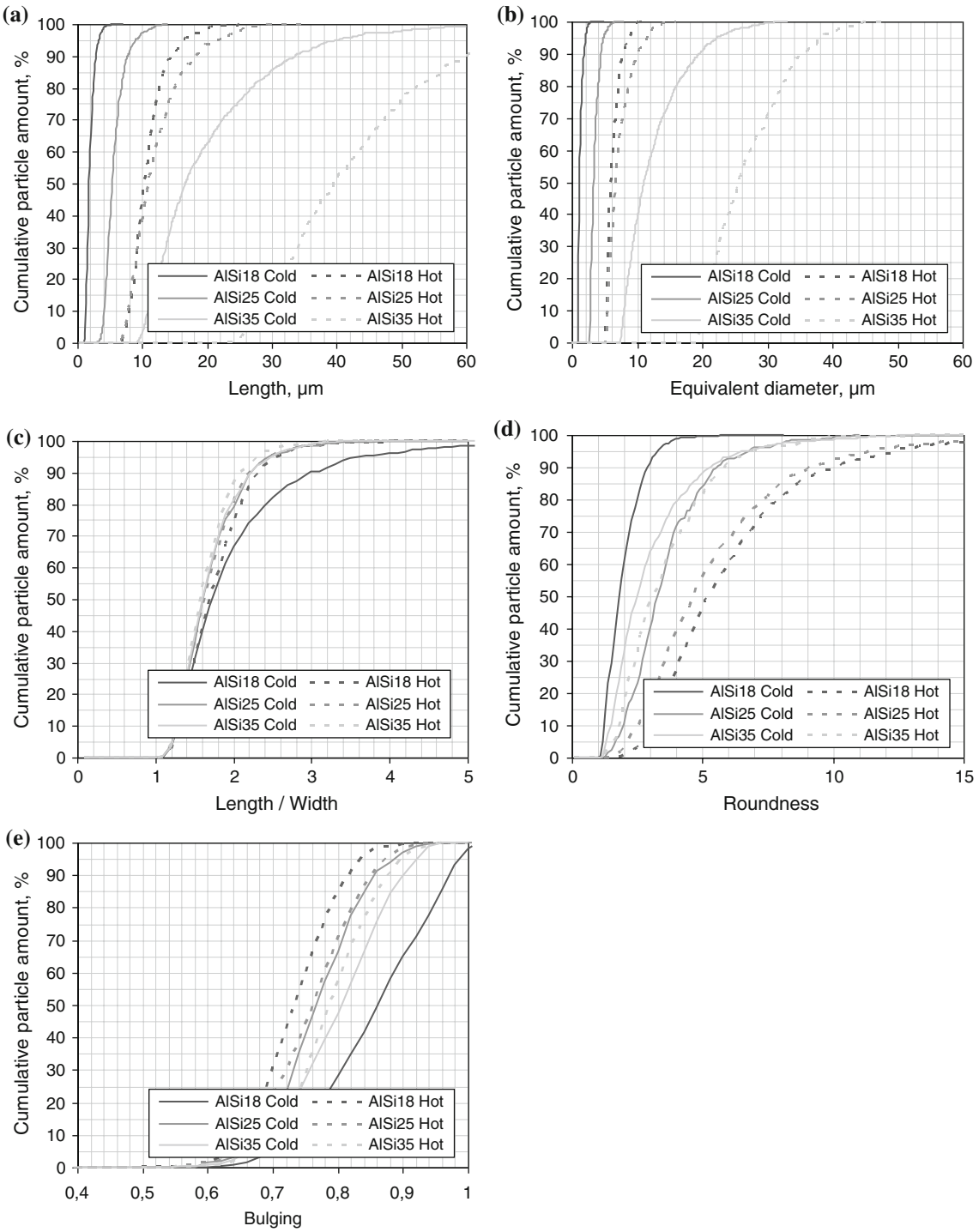

Fig. 7 Cumulative plots of size and shape of primary silicon in the as-deposited hypereutectic Al–Si alloys spray formed under different thermal conditions: **a** length, **b** equivalent diameter, **c** aspect ratio, **d** roundness, **e** bulging

AlSi25 deposit is around 10 and 11 μm, respectively, and the median particle length of the AlSi35 deposit reaches 40 μm. The extremely small silicon particles in the cold-sprayed AlSi18 deposit grow to a small extent after hot extrusion, but the large particles are sharply reduced in size due to particle facture during extrusion.

The equivalent diameter of the primary silicon particles shows the same tendency of change as the particle length. This parameter increases with increasing silicon content and thermal input in spray forming. For the cold-sprayed AlSi18, AlSi25 and AlSi35 deposits, the median equivalent diameter of the primary silicon particles is 1.1, 3.3 and

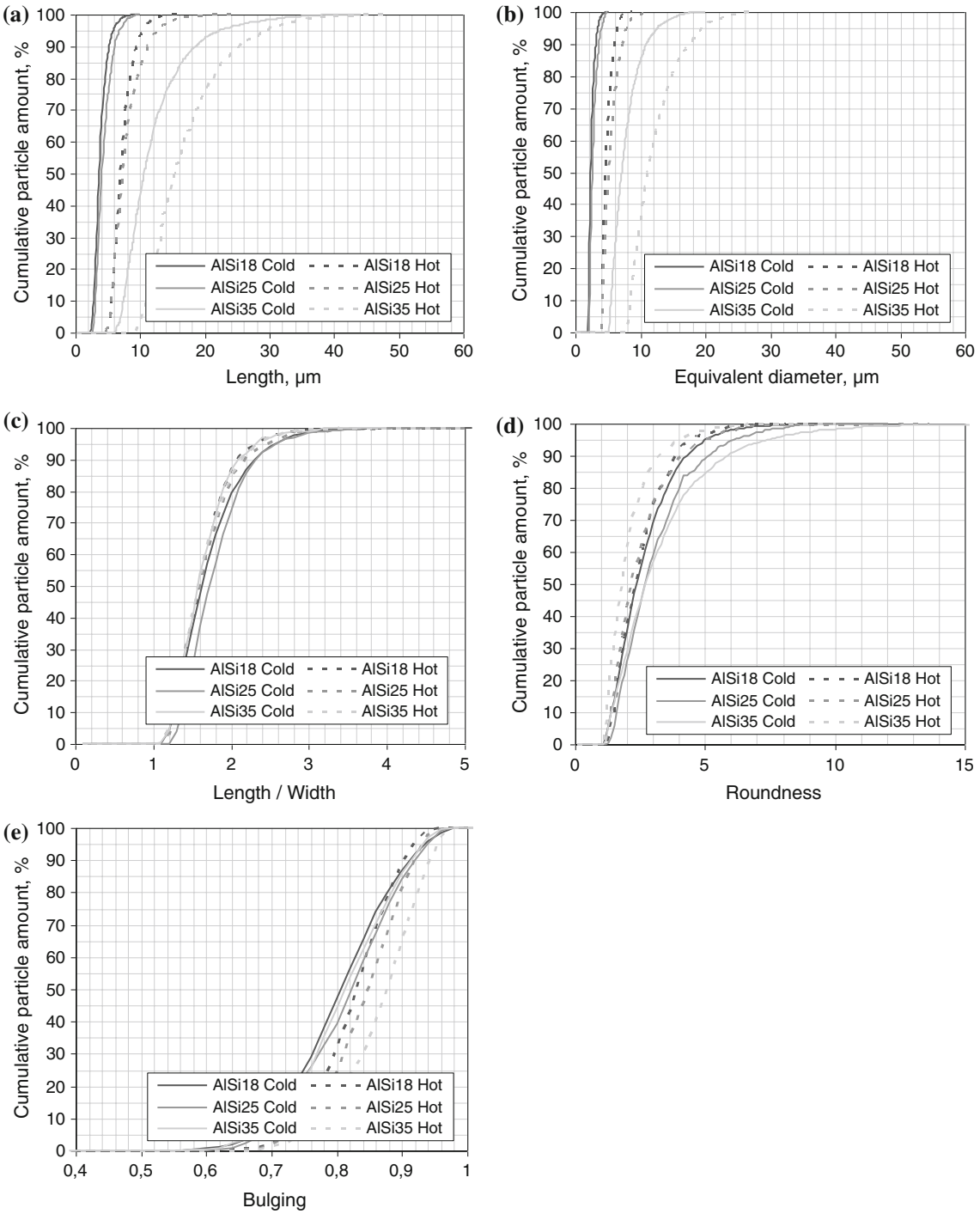

Fig. 8 Cumulative plots of size and shape of primary silicon in the as-extruded hypereutectic Al–Si alloys spray formed under different thermal conditions: **a** length, **b** equivalent diameter, **c** aspect ratio, **d** roundness, **e** bulging

11.1 μm, respectively. For the hot-sprayed AlSi18, AlSi25 and AlSi35 deposits, this parameter is 6.0, 6.7 and 25.6 μm, respectively. Extrusion changes the equivalent diameter of the primary silicon particles in AlSi35 significantly, since the silicon particles larger than 10 μm can fragment into small pieces. The particles smaller than 2 μm grow to a small extent, probably due to heating during extrusion. For the cold-sprayed AlSi18, AlSi25 and AlSi35 extrusions, the median equivalent diameter of the primary silicon particles is 2.4, 2.6 and 7.2 μm, respectively. For the hot-sprayed AlSi18, AlSi25 and AlSi35 extrusions, this parameter is 4.7, 5.1 and 11.1 μm, respectively. These measurements of the primary silicon particles by image analysis are in good agreement with the microscopic observation.

The median aspect ratio of the primary particles is also around 1.6, similar to that evaluated for all particles. Compared with the total particles (Fig. 5d), the primary silicon particles, particularly in the hot deposits, are less rounded and exhibit more pronounced bulging effect. The irregular shape of the primary particles may be explained by the preferential growth of the primary particles, especially under relatively slow cooling and solidification conditions. The influence of silicon content on the shape factors of the primary silicon particles is not obvious. Extrusion helps to make the primary silicon particles in the hot-sprayed alloys more regular in shape.

The distributions of the size factors and the shape factors of the primary silicon particles can be clearly illustrated by means of cumulative plots. The cumulative plots of the size factors and the shape factors of the primary silicon in the as-deposited hypereutectic Al–Si alloys spray formed under different thermal conditions and in the corresponding extrusions are given in Figs. 7 and 8, respectively. The distribution patterns of these factors tend to be more consistent after extrusion.

Interparticle spacing

The interparticle spacings of all silicon precipitates in the as-deposited hypereutectic Al–Si alloys spray formed under different thermal conditions as well as in the corresponding as-extruded alloys are compared in Fig. 9. The interparticle spacing of the silicon particles, over the range from 2 to 10 μm, increases with increasing silicon content in the deposits and thermal conditions during spray forming. This can be attributed to the different numbers of silicon precipitates in the deposits (see Fig. 4). Large particle quantity suggests high degree of dispersion of the particles. Hot spray conditions lead to large interparticle spacing due to low nucleation rate and coarsening of the silicon phases in the slow cooling and solidification process. As an exception, the comparatively small interparticle spacing of the hot-sprayed AlSi35 alloy can be explained

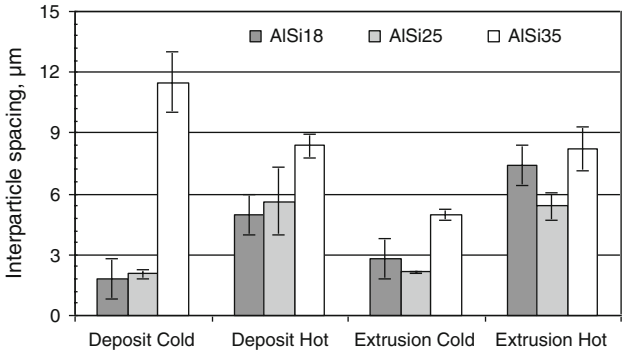

Fig. 9 Interparticle spacing of all silicon precipitates in the as-deposited and as-extruded hypereutectic Al–Si alloys spray formed under different thermal conditions

by the presence of acicular eutectic between the primary silicon particles. The interparticle spacing of the silicon phases in the as-extruded AlSi18 alloy is larger than that in the as-deposited AlSi18 alloy since the fine silicon particles in this alloy may coarsen to some extent during hot extrusion. The interparticle spacing of the particles in the AlSi25 alloy shows no apparent change after extrusion. The interparticle spacing of the particles in the cold-sprayed AlS35 alloy decreases after extrusion since the silicon particles fracture and redistribute in the α-aluminium matrix during deformation.

Anisotropy factors and orientation

The anisotropy factors of all silicon particles in the as-deposited hypereutectic Al–Si alloys spray formed under different thermal conditions and in the corresponding as-extruded alloys are compared in Fig. 10. The silicon particles in the as-deposited alloys show very small amount of anisotropy. The anisotropy factors of the silicon particles increase obviously after extrusion. It tends to decrease with increasing silicon content.

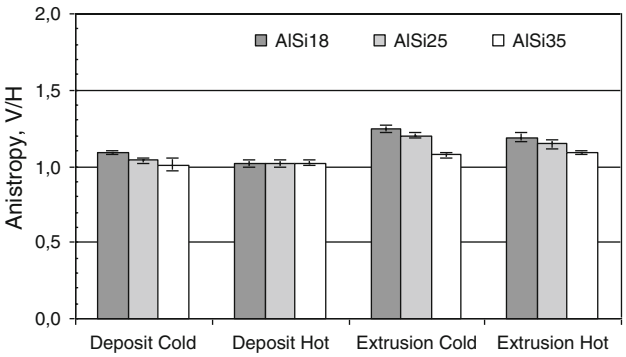

Fig. 10 Anisotropy factors of all silicon precipitates in the as-deposited and as-extruded hypereutectic Al–Si alloys spray formed under different thermal conditions

Figure 11 presents the orientation of all silicon precipitates in the deposits and in the extrusions. The silicon particles in the alloys show random orientation in the deposits; however, a low level of orientation towards the extrusion direction is found after extrusion. This is probably due to the deflection of the elongated particles in the preferred direction with the material flow during deformation, which also accounts for the anisotropy of the particles in the extrusions. The significance of the orientation decreases with increasing silicon content since the large particles fracture into small particles having a more regular shape.

Conclusions

Image analysis method was used to characterize quantitatively the silicon particles of the spray-formed and extruded hypereutectic Al–Si alloys and find the differences in the alloys prepared under different processing conditions. The main results can be summarized as follows:

1 The silicon particles are greatly refined and uniformly distributed in the spray-formed Al–Si alloys. This improvement in the silicon phases is further facilitated

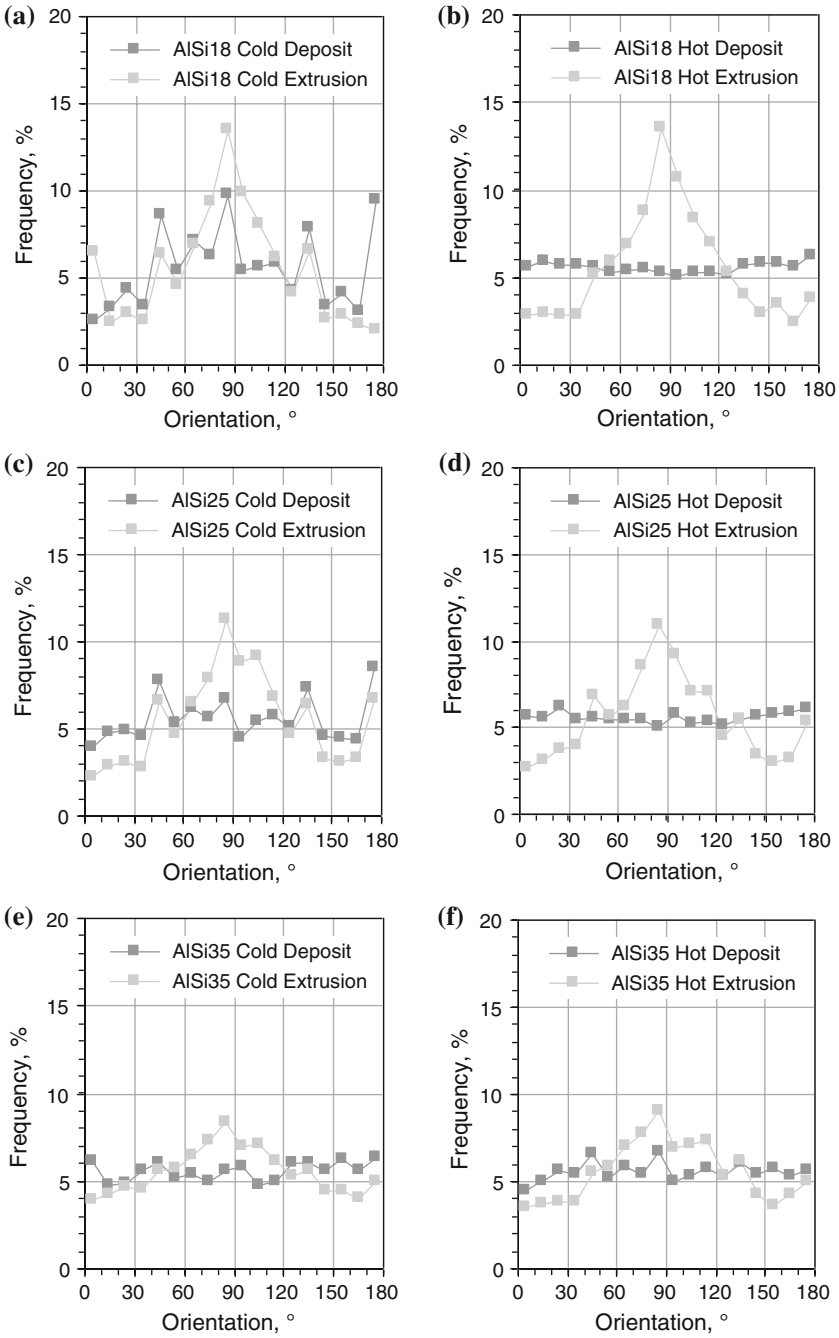

Fig. 11 Orientation of all silicon precipitates in the as-deposited and as-extruded hypereutectic Al–Si alloys spray formed under different thermal conditions: **a** AlSi18, cold sprayed, **b** AlSi18, hot sprayed, **c** AlSi25, cold sprayed, **d** AlSi25, hot sprayed, **e** AlSi35, cold sprayed, **f** AlSi35, hot sprayed

by low thermal input (decreased silicon content) as well as fast cooling conditions during spray forming. The silicon particles, depending on the particle size and shape, may fracture or coarsen during extrusion.

2 The areal density of the silicon particles decreases with increasing silicon content and associated enthalpy input in the deposits. Fast cooling conditions also lead to high areal density of the silicon particles.

3 The interparticle spacing of the silicon phases increases with increasing silicon content and decreasing cooling rate during spray forming. Extrusion plays a role on the interparticle spacing according to particle growth or fragmentation mechanisms.

4 The primary silicon particles in the hot-sprayed deposits are less rounded compared to those in the cold-sprayed deposits. The silicon particles in the as-extruded Al–Si alloys appear more homogeneous and regular than those in the as-deposited Al–Si alloys but exhibit a certain amount of anisotropy and a tendency to preferred orientation.

Acknowledgements The authors gratefully acknowledge the financial support of the German Federation of Industrial Research Associations "Otto von Guericke" (AiF, Die Arbeitsgemeinschaft industrieller Forschungsvereinigungen "Otto von Guericke" e.V.) within the program AiF-19ZN at the Foundation Institute for Materials Science (IWT) in Bremen. We would also like to thank our project partners for their beneficial contributions and valuable discussions.

References

1. Hatch JE (1984) Aluminium, properties and physical metallurgy. American Society for Metals, Metals Park, OH
2. Hegde S, Prabhu KN (2008) J Mater Sci 43(9):3009. doi: 10.1007/s10853-008-2505-5
3. Wu Y, Cassada WA, Lavernia EJ (1995) Metall Mater Trans 26: A1235
4. Yamauchi I, Ohnaka I, Kawamoto S, Fukusako T (1986) Trans Jpn Inst Met 27:195
5. Hogg SC, Atkinson HV (2005) Metall Mater Trans 36:A149
6. Lawley A (2000) In: Bauckhage K, Uhlenwinkel V, Fritsching U (eds) Spray deposition and melt atomization (SDMA). Bremen, Germany, p 3
7. Lavernia EJ, Wu Y (1996) Spray atomization and deposition. Wiley, New York
8. Leatham A (1996) Mater World 4(6):317
9. Chiang CH, Tsao CYA (2006) Mater Sci Eng 417:A90
10. Ha TK, Park WJ, Ahn S, Chang YW (2002) J Mater Proc Technol 130–131:691
11. Grant PS (2007) Metall Mater Trans 38:A1520
12. Raju K, Ojha SN, Harsha AP (2008) J Mater Sci 43(8):2509. doi: 10.1007/s10853-008-2464-x
13. Kainer KU (2006) Metal matrix composites. Wiley-VCH Verlag GmbH & Co. KGaA, Weinheim
14. Hogg SC, Lambourne A, Ogilvy A, Grant PS (2006) Scr Mater 55:111
15. Liang X, Lavernia EJ (1994) Metall Mater Trans 25:A2341
16. Cui C, Schulz A, Buschenhenke F, Seefeld T (2008) Entwicklung von Schweißzusatzwerkstoffen durch Sprühkompaktieren zur Verbesserung der Nahteigenschaften bei hochfesten Aluminiumwerkstoffen, Final report of the research project AiF ZuTech 191 ZN supported by the German Federation of Industrial Research Associations "Otto von Guericke" (AiF, Die Arbeitsgemeinschaft industrieller Forschungsvereinigungen "Otto von Guericke" e.V.), p 12
17. Cui C, Schulz A, Schimanski K, Zoch H.-W, Baumgart P, Syassen F, Kocik R (2007) In: Vollertsen F, Thomy C (eds) Proceedings of the international conference on applied production technology (APT'07), Bremen, Germany, p 123
18. Leica QWin, Reference manual 1997
19. Exner HE (1993) Prakt Metallogr 30:216
20. Stockham JD, Fochtman EG (1977) Particle size analysis. Ann Arbor Science Publishers, Ann Arbor
21. Russ JC (1999) The image processing handbook, 3rd edn. CRC Press LLC, Boca Raton, FL
22. Bouwman AM, Bosma JC, Vonk P, Wesselingh JA, Frijlink HW (2004) Powder Technol 146:66
23. Nikolakakis I, Kachrimanis K, Malamataris S (2000) Int J Pharm 201:79
24. Karnezis PA, Durrant G, Cantor B (1998) Mater Charact 40:97
25. Xu CL, Yang YF, Wang HY, Jiang QC (2007) J Mater Sci 42(15):6331. doi:10.1007/s10853-006-1189-y
26. Cui C, Schulz A, Schimanski K, Zoch HW (2009) J Mater Proc Technol 209:5220
27. Birol Y (2008) J Mater Sci 43(10):3577. doi:10.1007/s10853-008-2565-6